



HAL
open science

Localized Enzyme-Assisted Self-Assembly of low molecular weight hydrogelators. Mechanism, applications and perspectives

Cyprien Muller, Aymeric Ontani, Alexis Bigo-Simon, Pierre Schaaf, Loïc Jierry

► To cite this version:

Cyprien Muller, Aymeric Ontani, Alexis Bigo-Simon, Pierre Schaaf, Loïc Jierry. Localized Enzyme-Assisted Self-Assembly of low molecular weight hydrogelators. Mechanism, applications and perspectives. *Advances in Colloid and Interface Science*, 2022, 304, pp.102660. 10.1016/j.cis.2022.102660 . hal-03669764

HAL Id: hal-03669764

<https://hal.science/hal-03669764v1>

Submitted on 22 Jul 2024

HAL is a multi-disciplinary open access archive for the deposit and dissemination of scientific research documents, whether they are published or not. The documents may come from teaching and research institutions in France or abroad, or from public or private research centers.

L'archive ouverte pluridisciplinaire **HAL**, est destinée au dépôt et à la diffusion de documents scientifiques de niveau recherche, publiés ou non, émanant des établissements d'enseignement et de recherche français ou étrangers, des laboratoires publics ou privés.



Distributed under a Creative Commons Attribution - NonCommercial 4.0 International License

Localized Enzyme-Assisted Self-Assembly of low molecular weight hydrogelators. Mechanism, applications and perspectives

Cyprien Muller,^a Aymeric Ontani,^a Alexis Bigo--Simon,^{a,b} Pierre Schaaf^{*a,c} and Loïc Jierry^{*a}

^a *Université de Strasbourg, CNRS, Institut Charles Sadron (UPR22), 23 rue du Loess, 67034 Strasbourg Cedex 2, BP 84047, France.*

^b *Université de Strasbourg, Faculté de Chimie, UMR7140, 1 rue Blaise Pascal, 67008 Strasbourg Cedex.*

^c *Institut National de la Santé et de la Recherche Médicale, INSERM Unité 1121, CRBS, 1 rue Eugène Boeckel, 67085 Strasbourg Cedex, France.*

Pierre Schaaf: schaaf@unistra.fr

Loïc Jierry : ljierry@unistra.fr

Abstract

Nature uses systems of high complexity coordinated by the precise spatial and temporal control of associated processes, working from the molecular to the macroscopic scale. This living organization is mainly ensured by enzymatic actions. Herein, we review the concept of Localized Enzyme-Assisted Self-Assembly (LEASA). It is defined and presented as a straightforward and insightful strategy to achieve high levels of control in artificial systems. Indeed, the use of immobilized enzymes to drive self-assembly events leads not only to the local formation of supramolecular structures but also to tune their kinetics and their morphologies. The possibility to design tailored complex systems taking advantage of self-assembled networks through their inherent and emergent properties offers new perspectives for the design of novel, more adaptable materials. As a result, some applications have already been developed and are gathered in this review. Finally, challenges and perspectives of LEASA are introduced and discussed.

Keywords

hydrogels, enzyme, self-assembly, spatiotemporal control, low molecular weight hydrogelator.

TOC

LEASA, a powerful tool to spatiotemporally control supramolecular hydrogels.

Content of paper

Introduction

1 – Mechanism of Enzyme-Assisted Self-Assembly of LMWH

- 1-1 There exist four different types of Enzyme-Assisted Self-Assembly (EASA) processes
- 1-2 EASA kinetics present a lag time before self-assembly starts. Influence of the precursor's aggregation on the self-assembly process
- 1-3 Do molecular assemblies of LMWH present a long-range order?
- 1-4 Where does the EASA process start?
- 1-5 Do proteins or enzymes influence the 3D organization of the self-assembled structure?
- 1-6 Self-assembled structures are out-of-equilibrium structures
- 1-7 Enzymes seem to be incorporated in the peptide self-assembled network
- 1-8 Do self-assembled hydrogelators be in equilibrium with free hydrogelators in the hydrogel?
- 1-9 Mechanism of EASA: summary of what we know and do not know yet

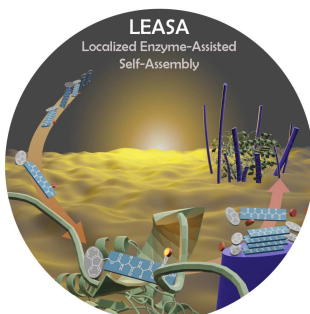
2 – Localized Enzyme-Assisted Self-Assembly

- 2-1 LEASA processes on macroscopic planar surfaces
- 2-2 Protein-assisted self-assembly localized on surfaces
- 2.3 Localized self-assemblies triggered by non-covalently attached enzymes can reach several micrometers thicknesses and are often oriented
- 2-4 LEASA processes on nanoparticles
- 2-5 LEASA processes in host gels

3. Applications of LEASA

- 3.1. Design of smart materials
- 3.2. LEASA for the design of catalytic systems
 - 3.2.a. LEASA allows the design of supported-hydrogels in flow reactors
 - 3.2.b. Design of localized supramolecular autocatalytic systems
- 3.3. Biomedical developments

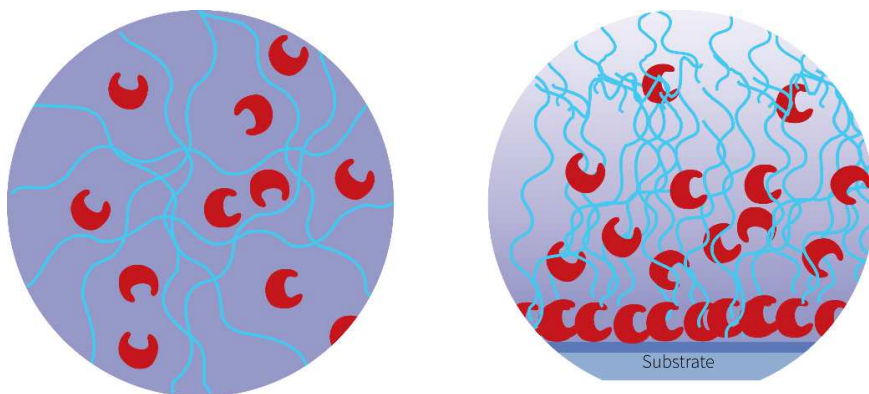
4. Perspectives for LEASA



References

Introduction

Biological cells are chemical systems controlled by tremendous complex interplaying of chemical reactions and physico-chemical processes, conferring them an extraordinary capability to respond to external stimuli at various scales. Most of these reactions and processes are triggered and regulated by enzymes. Cells are also physico-chemical systems where self-assemblies play a major role. Actin filaments which are of primary importance in cell motility are a typical example of such self-assemblies. Their appearance, dynamics and localization are governed enzymatically. In 2004, in an effort to provide a new way to get hydrogels, Bing Xu introduced the concept of *enzyme-assisted self-assembly* (EASA) of low molecular weight hydrogelators (LMWH)[1]. This concept mimics self-assembly processes taking place in cells. In this work, a short (non-self-assembling) Fmoc-tyrosine phosphate, Fmoc-*p*Y (Fmoc = Fluorenylmethyloxycarbonyl; *p* = phosphate group; Y = tyrosine), precursor was dephosphorylated by alkaline phosphatase (AP) and the decrease in solubility of the resulting hydrogelator Fmoc-tyrosine (Fmoc-Y) drove the self-assembly which led to the formation of a gel. EASA is now an important tool used to develop both biocompatible hydrogels[2] and nanomaterials interacting with cells with potential applications in cancer therapy for example.[3-6] After the seminal work of Bing Xu, EASA was rapidly extended to other enzymes and hydrogelators, usually amphiphilic peptides [7]. Because the hydrogelators are generated by enzymes, their production can be spatially controlled by localizing the enzymes. This step has been taken by Ulijn in 2009 by grafting covalently the enzymes on surfaces and showing that self-assembly occurred on the surface [8]. Such processes, where the enzymes are localized, were called *localized enzyme-assisted self-assembly* (LEASA). [9] Localization can take place on a surface or in a 3D environment such as a host material (gel). LEASA processes were first described on cells in biological systems [10] even before introduced by Ulijn on surfaces. In this review we will focus on LEASA processes generated in synthetic systems and discard those described in biological systems which are widely covered by other reviews [11-13]. Because the description of LEASA processes requires a good understanding of the EASA's one, we will first critically discuss the main features of this latter and mention some of the issues still unanswered. We will base them on some illustrative examples without providing an extensive review of EASA. Then, an overview of the main developments based on LEASA will be outlined before discussing some of their recent applications.

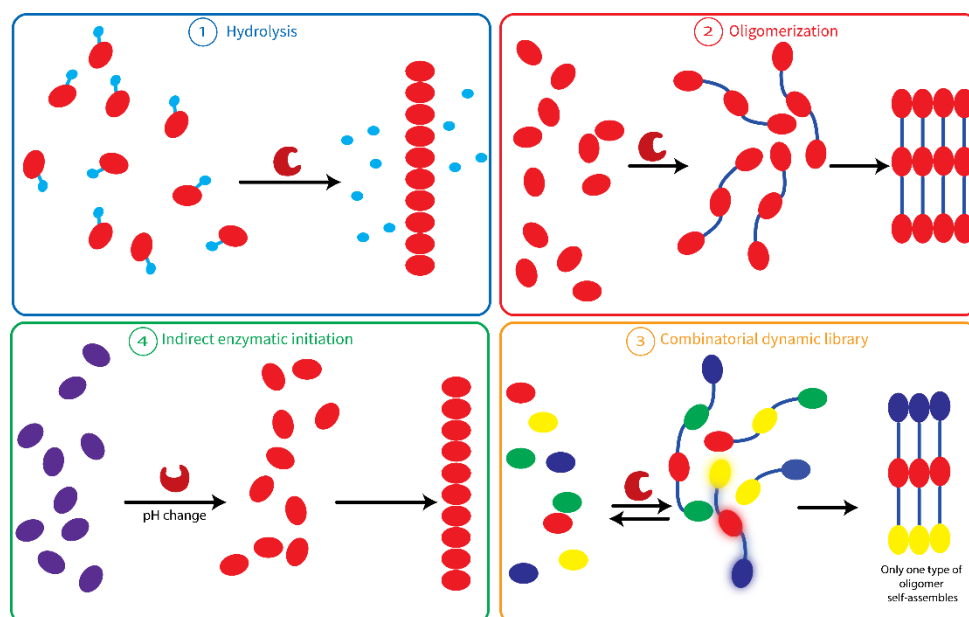


Scheme 1. Illustrations of (*left*) hydrogel generated from EASA, showing enzymes (red croissant) encapsulated in the LMWH self-assembly network (blue lines), and (*right*) hydrogel which grew from enzyme-localized surface (LEASA), highlighting the self-assembled nanofibers built from a bottom-up approach resulting in a distribution of the enzymes in the gel.

1 – Mechanism of Enzyme-Assisted Self-Assembly of LMWH

1-1 There exist four different types of Enzyme-Assisted Self-Assembly (EASA) processes

It can be distinguished four types of self-assemblies of LMWH induced by an enzymatic trigger (**Figure 1**). All of them are different by the way the enzyme generates the hydrogelator. The major part of papers in this field is based on the removal of a chemical group covalently linked to a precursor compound leading to the hydrogelator production. This is generally realized through the hydrolysis of ester, sugar or phosphate groups. This “catabolic” way has been introduced in 2004 by B. Xu in his pioneer work using a phosphatase to dephosphorylate a single tyrosine residue N-protected by a Fmoc group (Scheme 2.1) [1]. But EASA can also be involved in a tandem self-assembly process combining successively an enzymatic and then a chemical trigger. Indeed, Z. Yang and coll. reported a chemical system where AP transformed precursors into hydrogelator peptides that self-assembled into nanoparticles followed their self-assembly into nanofibers induced by the presence of glutathione.[14] An “anabolic” way has also been reported: in this case, the enzyme catalyzes the formation of the hydrogelator through the covalent bonding between two or several entities (Scheme 2.2). For instance, α -Chymotrypsin has been used to get an oligopeptide hydrogelator having an alternated sequence of polydipeptide (KL)_n from the KL ethyl ester precursor, KL-OEt (K=lysine; L=Leucine) [15]. In 2016, Ulijn and coworkers have illustrated another approach using thermolysin. This enzyme is able to catalyze the amides hydrolysis, their condensation and their exchange between various peptide sequences leading thus to a dynamic combinatorial peptide library (Scheme 2.3) [16] In this third case, it gives rise to selective amplification of the self-assembling peptide hydrogelators. Finally, the trigger of the LMWH self-assembly can also be realized through an indirect way, by switching the pH for instance. The addition of glucose to a mixture of glucose oxidase (GOx) and the dipeptide Fmoc-AA (A=alanine), results in a decrease of the pH which protonates the carboxylic group at the C-terminal position, leading to its self-assembly (Scheme 2.4).[17]



Scheme 2. Classification of the different EASA approaches reported in the literature in four categories. (1) Precursor (red ovals and blue spots linked together) compounds undergo the hydrolysis of a specific chemical group (blue spot) from the enzyme (croissant) action, releasing the hydrogelators (red ovals) which are self-assembling. (2) The enzyme (croissant) catalyzes the formation of oligomer hydrogelators which are self-assembling. (3) When the enzyme (croissant) is able to both link and disrupt different monomers (multicolored ovals) it leads to a dynamic combinatorial library of oligomers. The self-assembly of one of them displaces the equilibrium toward its predominance. (4) The enzyme (croissant) can change the pH and thus switch the charged state of precursors (dark blue ovals) to neutral hydrogelators (red ovals) which then are self-assembling.

1-2 EASA kinetics present a lag time before self-assembly starts. Influence of the precursor's aggregation on the self-assembly process.

Using reverse hydrolysis of peptide precursors by a proteolytic enzyme (thermolysin) which produces peptide hydrogelators through reverse hydrolysis capable of self-assembling into nanofibrillar structures, Williams *et al.* [18] examined the early stages of the EASA process of an Fmoc-trileucine (Fmoc-L₃) hydrogel from Fmoc-L and the dipeptide LL. At low enzyme concentration, using circular dichroism (CD) to monitor the self-assembly kinetics, they observed a short lag time between the enzymatic action and the self-assembly, which is inversely proportional to the enzyme concentration present in the solution. After this lag time, the self-assembly took place resulting in the formation of thin nanofibers whose entanglement ultimately led to the formation of a supramolecular hydrogel. Through a rheological study, Bing Xu and coworkers have reported a lag time of 10 minutes to form a gel from a Fmoc-*p*Y solution in presence of acid phosphatase used as enzyme. This period was attributed to the time necessary for the enzymes to produce enough hydrogelators (Fmoc-Y in this case) to initiate the self-assembly stage [19]. Using also Fmoc-*p*Y as precursor and AP as enzyme, Ulijn has established an EASA mechanism divided in three stages [20] first a rapid dephosphorylation of the precursor by AP, second the formation of aggregates of Fmoc-Y which then reorganize themselves in nanofibers and finally grow (Figure 1). The authors state that the aggregates are micelles characterized by their critical micellar concentration (cmc). Therefore, the kinetics of self-assembly through hydrolysis reactions present a lag time before self-assembly starts as well, highlighting thus a general feature of EASA, an observation also reported using enzymes generating the hydrogelators through oligomerization [9,15].

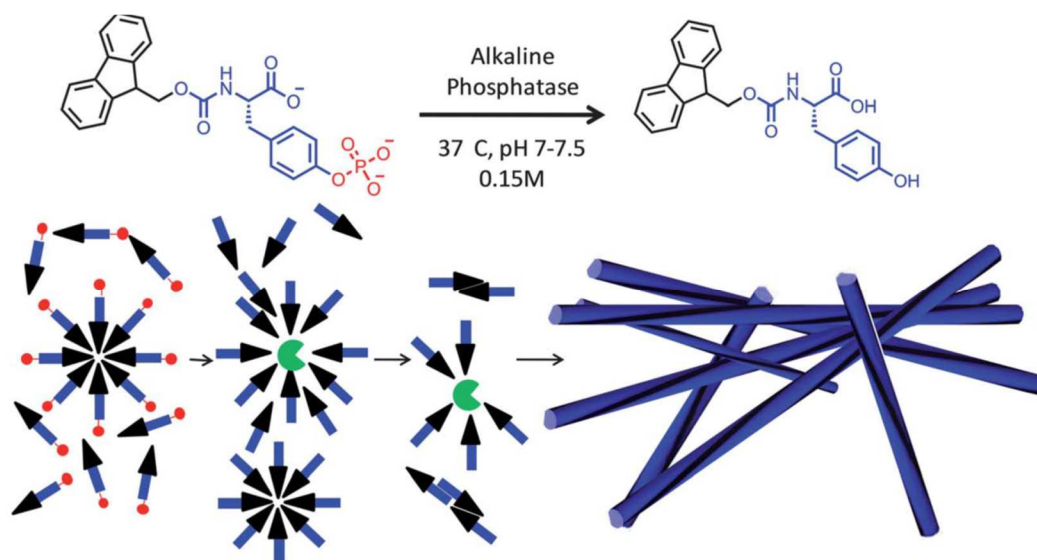


Figure 1. (Top) Enzymatic transformation of the precursor Fmoc-*p*Y into the hydrogelator Fmoc-Y in presence of AP. (Bottom) Proposed mechanism of the biocatalytic supramolecular transformation triggered by AP (green disk) in presence of the precursors (red spots-linked to the blue arrows). Reproduced from reference [20] with permission from the Royal Chemical Society.

Peptide self-assembly should thus also be influenced by the enzyme kinetics. This is exemplified by phosphatase triggered self-assembly. Most of the precursor peptides used in presence of AP contain phosphorylated residues. Bing Xu showed recently that AP reacts even faster with phosphorylated naphthyl and biphenyl moieties, leading to a faster self-assembly process.[21] The use of different motifs allows also the modulation of the morphology of the peptide self-assembly.

In most articles in the field, the description of the EASA mechanism assumes implicitly that the precursors are in a “free state” in solution before the enzymatic action, meaning fully hydrated. By using the peptide Fmoc-GFFYE-NH-(CH₂)₂-SS-(CH₂)₂-NHCO-(CH₂)₂-CO-EE-OH (SS=disulfide bridge) as precursor in presence of glutathione reductase, the hydrogelator Fmoc-GFFYE-NH-(CH₂)₂-SH is generated resulting in a supramolecular hydrogel [22]. Despite the full solubility of the precursor in water, we observed the absence of some ¹H NMR signals (measured in heavy water) indicating that this peptide is not free in solution but is rather in the form of aggregates. Addition of deuterated DMSO reveals all ¹H NMR signals. Using β-galactosidase to induce hydrogelation, it was reported that glycosylated precursors are organized in nanofibers before the enzymatic action, as observed by electronic microscopy [23]. This precursor organization was confirmed by contributions from Barthélémy and coll. [24]. As expected, similar conclusions arose from investigations about hydrogelation induced by other stimuli than the biocatalytic action [25]. Recently Zhimou Yang and coll. [26] studied the EASA of three N-Naphthalene (Nap) protected tripeptide precursors, Nap-*p*YYY, Nap-*Yp*YY and Nap-*YYp*Y, in the presence of AP. After the enzymatic dephosphorylation, all three precursors led to the same tripeptide Nap-*YYY* that has the ability to form a hydrogel. They observed that mixing Nap-*Yp*YY and AP at appropriate concentrations results in the formation of a hydrogel that is stable over time. On the other hand, mixing AP with the two other peptides, *i.e.* Nap-*p*YYY and Nap-*YYp*Y, leads to a slower formation of a weaker hydrogel resulting finally in precipitates. TEM images reveal that the gel deriving from Nap-*Yp*YY is constituted of thin micrometer-long nanofibers whereas with the other two peptides, the solutions contain a mixture of aggregates and small fibers. This different behavior cannot be charged to an assumed difference in the

dephosphorylation kinetics since they are almost all three identical after dephosphorylation, and are dephosphorylated in more than 98% after 1 hours in all cases. They also mention that the three phosphorylated peptides form micelles in solution and their cmc are 3181, 98, 1794 μM , respectively. The authors claim that the different behavior with respect to the self-assembly is due to a preorganization of the precursor aggregates in their phosphorylated state which then plays the role of critical nucleus for the self-assembly. Even if there is no direct proof of this, the conclusion seems reasonable. This again gives credit to the fact that the precursor peptides might be present in the form of aggregates. How these precursors interact with the enzymes and how these aggregates reorganize themselves or dissolve in the presence of the enzymes remains unknown.

1-3 Do molecular assemblies of LMWH present a long-range order?

The question here is to know if the fibers or other structures that are often observed in small peptide self-assemblies present an order over long distance. Using the dipeptide Fmoc-FF as hydrogelator, Smith et al. [27] have reported the formation of nanoribbons. They observed Bragg peaks corresponding to the presence of flat ribbons formed by parallelly aligned single fibrils along their long axis. A single peak corresponding to a distance of 4.3 Å and attributed to the distance between two Fmoc-FF dipeptides was also measured. Finally, the presence of a small peak at 16 Å is assigned to the spacing between two Fmoc groups (Figures 2a,b). Hughes et al. [28] investigated the hydrogelator Fmoc-SF-OMe which was generated *in situ* by mixing both Fmoc-S with F-OMe together in the presence of thermolysin. This resulted in the formation of 2D nano-sheets. The authors proposed lateral self-assembly forming extended arrays of β -sheets interlocked through π -stacking between Fmoc groups. This model was in accordance with WAXS spectra which exhibited peaks at 4.8 and 3.7 Å that were attributed to β -sheet spacing and π -stack spacing between the Fmoc groups. A prominent peak at 16 Å with several higher order reflections was also present which was attributed to repeating pattern along the peptide backbone. Yet these systems were all dried, which can eventually induce a long-range order. The question in the wet state is thus not answered.

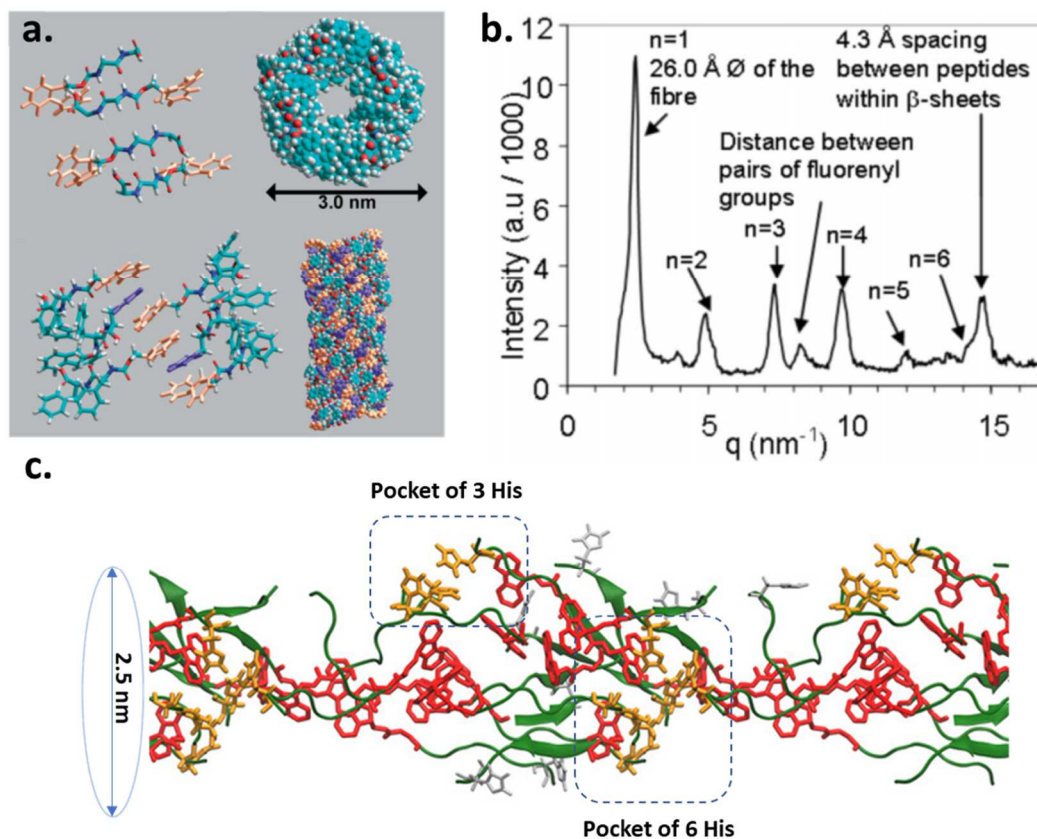


Figure 2. (a) Model structure of Fmoc-FF self-assembly arranged in an anti-parallel β -sheet pattern (Fmoc groups are colored in orange and phenyl groups of F residue in purple). (a) and (b) are reproduced from reference [27] with permission from Wiley-VCH. (c). Molecular dynamics of hydrogelators Fmoc-GFFYGHY showing a fiber-like spatial arrangement through 3D periodic boundary conditions (β -sheet structures are represented in green arrows, Fmoc moieties are in red, histidine involved in a hydrogen network are colored in yellow, the others in grey). Reproduced from reference [29] with permission from Wiley-VCH.

Molecular dynamic simulation (MDS) is a tool also used to elucidate the molecular organization of LMWH in the resulting nanostructures. Based on infrared spectroscopy and MDS studies, the hydrogelator (KL)₇, generated from KL-OEt in presence of α -chymotrypsin, appears to self-assemble in α -helices and β -sheets in a ratio depending on the initial concentration of the precursor dipeptide [9]. Furthermore, the esterase-like activity arising from the Fmoc-GFFYGHY peptide self-assembly, formed from the precursor Fmoc-GFFpYGHpY in presence of AP, was rationalized through MDS showing a catalytic pocket constituted of three to six histidine residues linked together through hydrogen bonds (Figure 2c).[29] This network enhanced the nucleophilicity of the imidazole groups involved in the catalytic activity.

Currently, the determination of 3D organizations almost at the atomic scale can be performed using the reconstruction images based on electronic microscopy technics with spectacular achievements of proteins structure [30]. Such developments appear highly suitable for the establishment of LMWH 3D structures in the future.

1-4 Where does the EASA process start?

Williams and Ulijn were the first to show that peptide self-assembly, initiated by enzymatic formation of the hydrogelator, starts where the enzyme is covalently grafted [8]. They immobilized covalently thermolysin on a surface and brought it in contact with a solution containing a mixture of Fmoc-L and L₂. Thermolysin catalyzed peptide bond

formation and formation of Fmoc-L₃ which self-assemble into nanofibrils. They observed, by TEM and AFM, that most of the fibers originated from small globules, typically 20-30 nm in width, which were attributed to enzyme clusters (Figures 3a,b). Yet one can also observe on their AFM image the formation of small fibrils that are not related to globules. Do these fibrils originate from single grafted enzymes not visible under AFM or do some fibrils form spontaneously from hydrogelators that are further away from the enzymes that produced them? Similar results were reported later using subtilisin which hydrolyzed O-methylated Fmoc-dipeptides, forming hydrogelators (Figure 3c) [31]. In this case too, the surface was covered by nanofibers and nanoclusters. Most of the fibers started from the clusters but there was also a large proportion of them that were not linked to nanofibers. Moreover, it is not yet clear what is the real nature of these nanoclusters: enzyme clusters or peptide clusters? This question should be further investigated. It should also be noticed that when the enzyme is adsorbed electrostatically on a surface and then brought in contact with an adequate precursor solution, globular and dense microstructures are formed quasi-spontaneously. Several microfibrils appear few minutes later, connecting the microstructures in a fibrous network. This time-lapse of events has been shown through AFM investigations using AP adsorbed on a surface in presence of the tripeptide Fmoc-FFpY (Figure 3d) [32]. Aspects concerning surface-induced EASA will be discussed in the next part of this review.

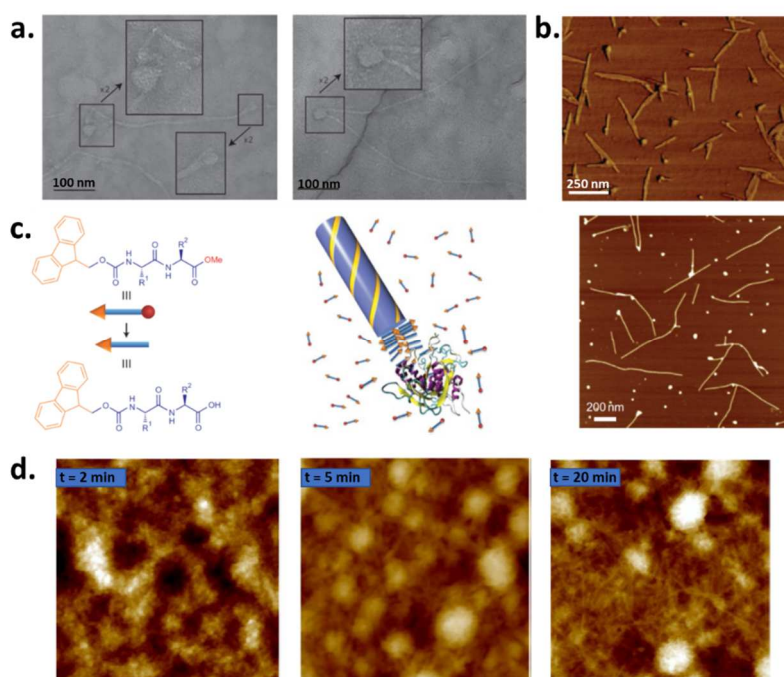


Figure 3. (a) TEM and (b) AFM images showing the peptide-self-assembled fibre growth from globular structures. Reproduced from reference [8] with permission from Springer Nature. (c) (from left to right) Chemical structure of Fmoc-dipeptide (Fmoc in orange, dipeptide sequence in blue and enzyme cleavable group in red), schematic of nucleation and growth in EASA and typical AFM image of the initial stage of self-assembly. Reproduced from reference [31] with permission from Springer Nature. (d) Typical AFM images (1 × 1 μm) taken over time (2, 5 and 20 minutes from left to right) from the contact between AP-adsorbed and Fmoc-FFpY solution. Reproduced from reference [32] with permission from Wiley-VCH.

1-5 Do proteins or enzymes influence the 3D organization of the self-assembled structure?

The observations mentioned in the above section 1-4 seem to indicate that the answer to this question is "yes". Li et al. [33] used Nap-GFFY-SS-EEE peptides (Nap=naphtyl group; SS=disulfide bridge) which, in the presence of dithiothreitol or glutathione formed a hydrogel that was not stable over times of the order of an hour. On the other hand, in the presence of bovine serum albumin (BSA) the gel became stable over days. Moreover G' and G'' of these gels increased as the BSA concentration increased, passed through a maximum at around 20 wt% before decreasing again. TEM revealed that the fiber network of the self-assembly changes with the concentration of BSA. With other proteins the stabilization of the gel was smaller. This seems to indicate direct interactions between the peptide hydrogelator and BSA and that these interactions have a strong influence on the self-assembled structure.

Based on the thermodynamic equilibrium between a peptide hydrogelator and its precursor (from thiol/disulfide equilibrium), our group has reported that the introduction of proteins can induce the increase of the hydrogelator content up to 100% resulting in gel formation [14]. According to the protein involved, the resulting nanostructures can be different: nanofibrils are obtained in the presence of glutathione reductase or AP, and platelets are obtained in the presence of albumin. The origin of these differences is not yet understood.

Jain et al. [34] studied the self-assembly of carboxybenzyl N-protected dipeptides Cbz-FL (Cbz=carboxybenzyl) which is a non-gelling peptide at room temperature. They brought Cbz-FY precursors in contact with different enzymes: a lipase (*Candida rugosa*), thermolysin and chymotrypsin. They observed an almost instantaneous gel formation in the presence of lipase, a slower gel formation (5 minutes) with thermolysin and no gel formation in the presence of chymotrypsin. Whereas with lipase, the self-assembly resulted in the formation of long thin fibers, fibers were much shorter in the presence of thermolysin and the presence of chymotrypsin resulted in the formation of aggregates observed by AFM. Using native and denaturated enzymes they showed that the self-assembly initiation does not depend on a specific interaction with proteins. This shows that the interaction between peptides and proteins can play a crucial role in the self-assembly initiation, certainly in the formation of the critical nucleation cluster for the self-assembly process. Are the fibers physically bound to the enzymes within the self-assembled gel remains an open question.

1-6 Self-assembled structures are out-of-equilibrium structures

LMWH self-assemblies can be obtained not only by an enzymatic trigger on a precursor but also by varying conditions such as the nature of the solvent or the temperature. In this case numerous studies reveal that for a given peptide, self-assembly depends upon the history of the sample [35,36]. Indeed, in the case of short peptides N-capped by an aromatic group, their self-assembly relies on the interplay of hydrogen bonds, hydrophobic and hydrophilic balance. All these interactions are temperature dependent [28,29]. For example, Debnath et al. [37] obtained different Fmoc-YL self-assembly organization by changing the thermal history of the sample. They heated a pre-formed self-assembled gel at various temperatures for 10 minutes before letting the sample cool back to room temperature. When heated above a temperature that corresponds to the melting temperature of β -sheet arrangements [38], they observed an inversion of the CD signal corresponding to the chiral supramolecular arrangement of the Fmoc moieties. Using NMR, they also found an overall greater amount of hydrogelators incorporated into the gel fibers when the temperature was raised. It must be reminded that all measurements were performed at room temperature and thus the samples kept the memory of the heating step. The influence of the thermal history of a gel on its structure and mechanical properties is extremely general and not restricted to

hydrogelators containing Fmoc moieties. Using NDB-GFFpY (NDB: nitrobenzoxadiazole) as precursor, Z. Yang and coll. found that contact with alkaline phosphatase at 37°C leads to the formation of nanoparticles whereas fibers form at 4°C. These structures are then observed at 20°C. Moreover the peptides in the fibers adopted an α -helix conformation whereas in the nanoparticles they showed a random coil conformation. These structural difference of the self-assembled NDB-GFFY peptides are attributed to both the influence of the temperature on the enzyme activity and on the diffusion processes in the system (Figure 4).[39]

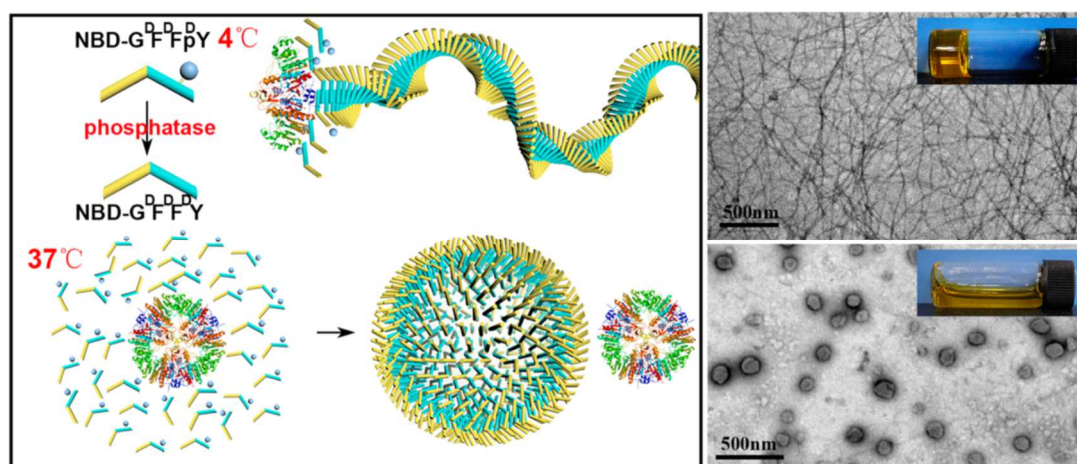


Figure 4. (left) Suggested model of molecular self-assembly of NBD-GFFFY (with non-natural chirality of the amino acids) from NBD-GFFpY and AP at 4°C or 37°C leading to (right) nanofibrous network (gel) or to peptide self-assembled nanoparticles (solution). Reprinted with permission from reference [39]. Copyrights 2022 from American Chemical Society.

Wang et al. observed that gels prepared from a mixture of 1,2,4,5-benzene tetracarboxylic acid and 4-hydroxypyridine by cooling the hydrogelator solution were constituted of fibers whose size decreased as a cooling speed was increased and the dynamic moduli G' and G'' increased [40]. Using Fmoc-FRGDF peptides, Li et al. [41] tuned the mechanical properties of the self-assembled hydrogels by changing the rate of change of the pH of the solution. The gels were composed of long nanofibers. A rapid change of the pH resulted in a network of smaller highly entangled fibers whereas a slow pH change led to a weaker gel composed nanofibrils that were aligned with few entanglements. On the other hand, the pH change did not affect the anti-parallel β -sheet structure of the fibers.

1-7 Enzymes seem to be incorporated in the peptide self-assembled network

The question of the incorporation of enzymes in self-assembled hydrogels could be critical for practical applications. Li et al. self-assembled Nap-GFFY-OMe hydrogelator from Nap-GFFpY-OMe precursor in presence of AP.[33] The resulting self-assembled hydrogel was washed with a phosphate buffer solution several times until no AP was detected in the washing solutions. Thus, the authors observed that the hydrogel remained enzymatically active which seems to indicate that AP is incorporated in the self-assembled network. Wang et al. [42] built gels using Fmoc-pY or Nap-FFpY and acid phosphatase. After gel formation they freeze-dried the gel and brought it in contact with organic solvents. The gel was highly catalytic and when in contact with water, only 12% of the enzymes were released. They did not specify if, for the experiments performed in water, the gel was first freeze-dried. On the other hand, when the hydrogel was formed starting directly from the hydrogelator Fmoc-Y through heating and cooling steps, and then brought in contact with an enzyme solution, the content of enzymes adsorbed in the gel corresponded to only 8% of the amount found in the hydrogel built enzymatically. They concluded that the enzymes inducing the self-assembly

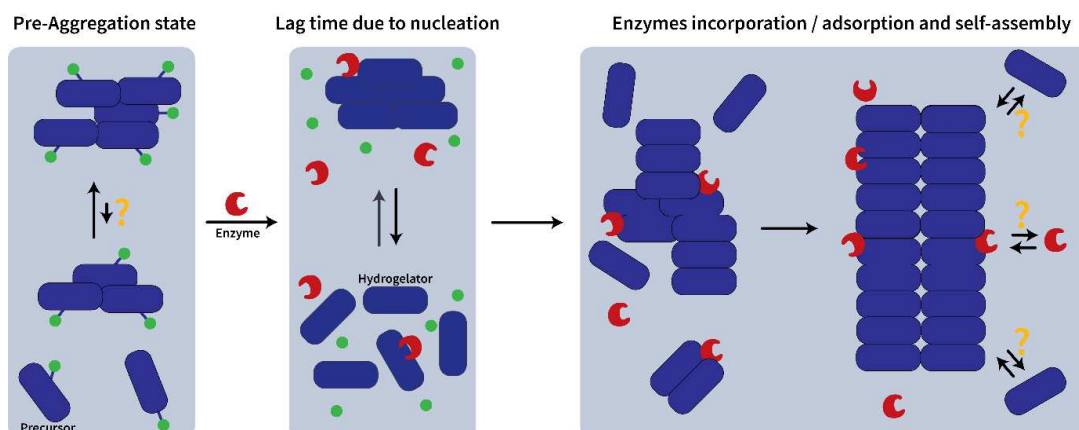
are incorporated in or strongly adsorbed on the fibers during the self-assembly process. On the other hand, enzymes that were brought in contact with the fibers after their buildup only weakly bound to them.

1-8 Do self-assembled hydrogelators be in equilibrium with free hydrogelators in the hydrogel?

The question of the equilibrium between free and assembled peptides was very seldom addressed. To our knowledge only two studies try to get an answer to this question. First, experiments performed by Roy and Ulijn [43] determined the concentration of free peptide hydrogelators present in a self-assembled hydrogel. This was done by first determining the partition coefficient of these peptides between an aqueous solution and diethyl ether under small peptide concentrations. Once the coefficient was determined, they brought a self-assembled gel in contact with diethyl ether, let equilibrium between the two phases take place and then measured the concentration of peptides in the organic phase. Using the hydrogelator peptide Fmoc-YL in the presence of different ions, they found that between 5 and 8% of the peptides present in the self-assembled gel are free peptides, depending on the place of the ion in the Hofmeister series. This seems to indicate that there exists an equilibrium between the peptides in the self-assemblies and free peptides. Yet it could also be that during the self-assembly buildup some peptides did not enter the self-assemblies due to self-assembly kinetics. Experiments were not performed by increasing, for example the volume of the organic phase, which could lead to a reduction of the self-assembly kinetics. Another experiment realized by the group of Bing Xu [44] seems to indicate that there exists, indeed, an equilibrium between peptides in the self-assembled state and free peptides. In these experiments, peptides were designed to be able to interact reversibly with a small ligand (vancomycin). The peptides that are associated with the ligands could not self-assemble in the form of nanofibers and the ligands could not associate with the peptides inserted in the self-assembled fibers. Now, when the fibers were first self-assembled in the absence of ligands and then ligands were added in a large amount (1:4 ligand:peptide molar ratio) the fibers disassembled, and the gel became a cloudy solution. This proves that peptides involved in self-assembled fibers can leave the fibers and thus are in equilibrium with free peptides. These then interact with ligands, displacing the equilibrium towards disassembly of the fibers. The question is to know if this conclusion can be extended to all peptide self-assembled hydrogels? Indeed, as will be discussed later, Fmoc-GFFYGHY hydrogels constructed on the walls of a porous material are stable under flow of aqueous solutions through the material for long time (several days).[45] This seems to contradict the existence of an equilibrium between free and self-assembled peptides.

1-9 Mechanism of EASA: summary of what we know and do not know yet.

Taking into account all the points discussed above, a general mechanism of the EASA process is proposed in Scheme 3. This mechanism is based on a precursor undergoing a chemical hydrolysis (phosphate group hydrolysis, ester hydrolysis, etc), in presence of the suitable enzyme, resulting in the generation of hydrogelators. Three main stages can be distinguished: the pre-aggregation state, the nucleation step and finally the hydrogelator self-assembly. The complexity of the EASA process and remaining questions are highlighted.



Scheme 3. General mechanism pathway of EASA using precursor compounds (blue rectangle) including a chemical group (green spot) which is cleavable through the action of suitable enzymes (red crosses). This leads to the formation of the hydrogelators (blue rectangles). Question marks indicate open questions.

2 – Localized Enzyme-Assisted Self-Assembly

2-1 LEASA processes on macroscopic planar surfaces

As already mentioned before, the first example of LEASA was reported by Ulijn in 2009, introducing so the concept [8]. Amide bond formation between Fmoc-protected amino acid precursors and nucleophilic dipeptides leads to a combinatorial constitution of hydrogelators. First, the study proved the reaction to be catalyzed by the presence of thermolysin in solution. When the enzyme was covalently attached to an adequately substituted glass substrate, which was then dipped into a solution containing the precursors, formation of self-assembled structures was observed on the thermolysin-modified surface thus proving that the immobilization of enzymes on a surface results in localization of self-assembly near the enzymes, as observed by transmission electron microscopy (TEM) and atomic force microscopy (AFM) (Figures 3a,b). The resulting fibres nucleate and grow from spheres of approximately 20-30 nm in diameter. As the nucleation process is mostly thought to occur around enzyme molecules, these spherical objects were attributed to enzyme aggregates but, as already discussed, these particles could also be small peptide aggregates.

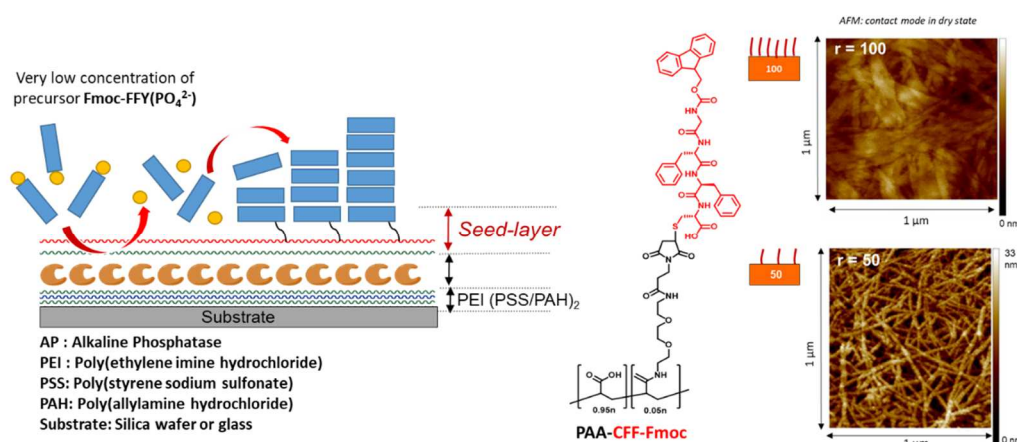


Figure 5. (Left) Schematic of AP adsorbed in a polyelectrolyte multilayer film and dephosphorylation of Fmoc-FFpY leading to Fmoc-FFY self-assembly induced by the seed-layer. This latter is created through the adsorption on the top of the film of a modified PAA with the Fmoc-FF sequence. (Right) The relative density “r”

(100% or 50%) of the seeding polymer on the surface impacts the resulting nanoarchitecture of the supramolecular hydrogel. Reproduced from reference [32] with permission from Wiley-VCH.

Anchoring enzymes on a surface can easily be performed using polyelectrolyte multilayers [46] corresponding to a coating obtained by the alternate deposition of polyanions and polycations. Along this line we have introduced the concept of seed-layer to provide a LEASA system with controlled nucleation sites [32]. The surface was initially modified with an alkaline-phosphatase (AP)-containing polyelectrolyte multilayer onto which a peptide seed-layer was adsorbed (Figure 5). It was constituted of poly(acrylic acid) (PAA) modified by grafting 5% of the peptide sequence Fmoc-FF. Upon contact with this surface, the Fmoc-FFpY precursor peptides in solution can be dephosphorylated, thereby resulting in self-assembly starting from the seed-layer in about 10 minutes. Remarkable dependence was shown, as seed-layer led to much more deposition than the bare enzyme (*i.e.* AP) while sequence Fmoc-GGG grafted on PAA led to no self-assembly event. Accordingly, varying the surface density of seed-layer allowed tuning the fiber density at the surface. When high content of seed-layer was present on the surface, large ribbons were observed by atomic force microscopy (AFM) while lowering this content resulted in their disappearance. The thickness of the hydrogel reached, unexpectedly, up to ten microns. Such a large value of the thickness was explained by Ulijn's group by the non-covalent character of the enzyme deposition. Comparing LEASA processes initiated by thermolysin adsorbed or covalently linked on a glass substrate, they found that the latter led to much thicker films than the former [47]. This may be due to displacement of the non-covalently fixed enzymes during the self-assembly from the substrate into the self-assembled film where they can further induce self-assembly. From these observations, the authors developed a system where varying the ratio of bound (irreversibly immobilized) and unbound (reversibly immobilized) thermolysin on the glass surface allowed controlling the thickness of the gel from bulk to localized gelation of a Fmoc-TF dipeptide. Noteworthy, in the example of the seed layer, the amount of enzyme embedded in the seed-layer was quasi-linearly correlated to the kinetics of the self-assembly process, as expected from an earlier study on EASA [18].

Polyelectrolyte multilayers were also used to deposit α -chymotrypsin onto a surface. The enzyme then catalyzed the oligomerization of (KL)_n-OEt from dipeptide ethyl ester KL-OEt present in solution (K = lysine) [9]. The reaction was observed until a critical concentration of oligomer hydrogelators was reached, at which point self-assembly occurred. In this system, the self-assembly was ensured by a distribution of oligomers of different polymerization degrees n (up to $n=14$) that undergo self-assembly to yield nanofibers. By quartz crystal microbalance (QCM) monitoring, the systematic presence of a lag-time (typically a few minutes) before the start of the LEASA process was noticed. Interestingly, the kinetics could be tuned in two ways (*i*) by increasing the concentration in KL-OEt precursor and (*ii*) by lowering enzyme surface density, respectively decreasing and increasing the lag time. Such a result is well in agreement with the hypothesis that the lag time is proportional to the rate at which the LMWH may accumulate, as stated in a study discussed earlier [18]. These examples show that LEASA is a viable strategy to obtain time-control over self-assembly processes even if temporal-control of the self-assembly process remains a challenge.

A more typical approach for the spatiotemporal control of self-assembly events at a surface is the use electrodes through the electro-generation of protons [48]. In 2017, this

approach was mimicked *via* LEASA with the intention to extend such a strategy to non-conductive surfaces (and therefore beyond electrode material) [17]. In this work, the use of glucose oxidase deposited on a polyelectrolyte multilayer allowed to generate enzymatically a proton gradient emanating from the surface in the presence of oxygen (Figure 6). As expected, the localized decrease of pH enabled the protonation of the carboxylic acid at C-term position of the Fmoc-AA dipeptide precursor (A = alanine), resulting in self-assembly near the surface by rendering the peptide less charged and polar. Interestingly, this strategy was also extended to deoxygenated solutions by addition of a horseradish peroxidase (HRP) layer that could catalyze the transformation of hydrogen peroxide to oxygen, thereby fueling the system. These results are highly important because they show the wider variety of surfaces that can be used in LEASA. Moreover, this strategy differs from all other LEASA studies as the enzymatic activity acts to create a morphogen (by only controlling local conditions) and is therefore indirectly responsible for the self-assembly.

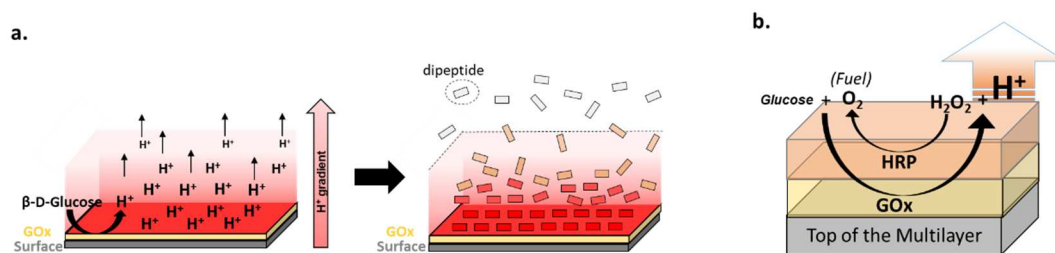


Figure 6. (a) Schematic of LEASA based on the enzymatic production of a protons gradient due to the oxidation of glucose by GOx. This protons gradient directs the self-assembly of the dipeptide Fmoc-AA. (b) To ensure a continuous supply in dioxygen (O₂) required by GOx, an additional layer of HRP is adsorbed. This enzyme transforms the second product H₂O₂ generated GOx, into O₂ in a sustainable way. Reproduced from reference [17] with permission from Wiley-VCH.

We thus see that each of the three EASA processes, namely hydrolysis reactions, reverse hydrolysis reactions and activation of the hydrogelators through morphogens (*i.e.* protons), can efficiently be translated into a LEASA process.

2-2 Protein-assisted self-assembly localized on surfaces

Up to now we have discussed self-assembly processes where the hydrogelator was produced enzymatically from a non-self-assembling small molecule precursor. As already mentioned [22], non-catalytic proteins can also, in special cases, induce local self-assembly. The reversible cleavage of a disulfide bridge (SS) protecting a pentapeptide Fmoc-GFFYE-SS-EE (precursor) into Fmoc-GFFYE-SH (hydrogelator) and HS-EE was first investigated, in solution, in the presence of bovine serum albumin (BSA) and catalytically active proteins, such as AP, which do not play their role of enzymes toward the precursor. To further study the self-assembly mechanism, the different proteins were immobilized on gold substrates using polyelectrolyte multilayer films. The protein deposition and the self-assembled hydrogel growth on surfaces were monitored by QCM. Interestingly, when no enzyme was immobilized and the surface of the polyelectrolyte was charged positively by using poly-L-lysine as an external layer, similar deposition was observed than with proteins. This indicates that the main driving force for this self-assembly event is the electrostatic interaction. Such a structuring effect from a protein onto the self-assembled network was also observed in earlier works by Williams [49]: addition of a non-catalytic protein, laminin, caused a sharp increase in the level of conversion to a tripeptide hydrogelator. This result is expected to rise from

electrostatic interactions between hydrogelators and laminin that would promote the amide bond formation, a hypothesis further supported by the increased supramolecular order in the presence of the protein. Indeed, CD showed an increase in chirality while rheology revealed storage moduli stronger by one order of magnitude and TEM showed bundles formation (Figure 7).

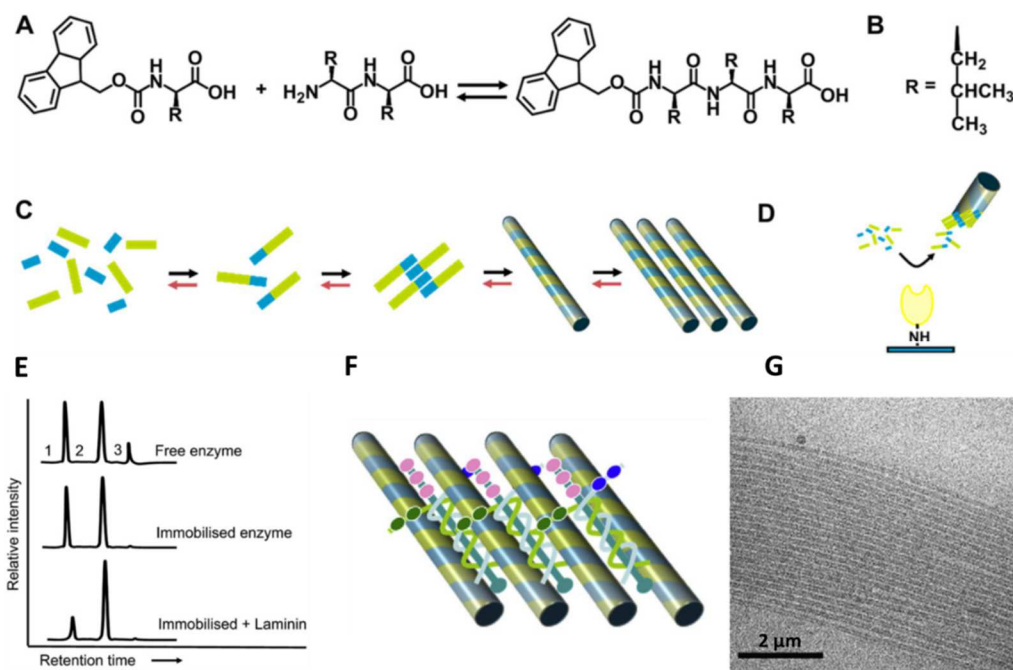


Figure 7. (a,b) Equilibrium between the precursors Fmoc-L and the dipeptide LL ensured by thermolysin, leading to the formation of the hydrogelator Fmoc-L₃ (among other peptides). (c) Schematic of the formation of the hydrogelator Fmoc-LLL from Fmoc-L (blue) and dipeptide LL (green) resulting in longitudinal nanofibers. (d) When thermolysin is immobilized, the hydrogelator Fmoc-L₃ hydrogelator self-assembles near the surface. (e) HPLC chromatogram: 1 corresponds to Fmoc-L, 2 to Fmoc-L₃ and 3 to Fmoc-L₅. (f) Schematic of Fmoc-L₃ nanofibers interacting with laminin. (g) Bundles of nanofibers observed by cryo-TEM. Reproduced from reference [49] with permission from Elsevier.

2.3 Localized self-assemblies triggered by non-covalently attached enzymes can reach several micrometers thicknesses and are often oriented.

In all cases where the enzyme or proteins were deposited on the surface through a polyelectrolyte multilayer, the self-assembled layers reached up to several tens of micrometers. In some cases, a density gradient of nanofibers showed up. This was evidenced by cryo-scanning electron microscopy (cryo-SEM, Figure 8) [29]. It also appeared that fiber growth occurs mostly perpendicularly to the substrate. A similar observation was made for non-biocatalytic triggers as well [50]. Up to now there is no clear explanation for this orientation. In addition, a higher density of fibers is present near the substrate-hydrogel interface than on the top of the hydrogel.

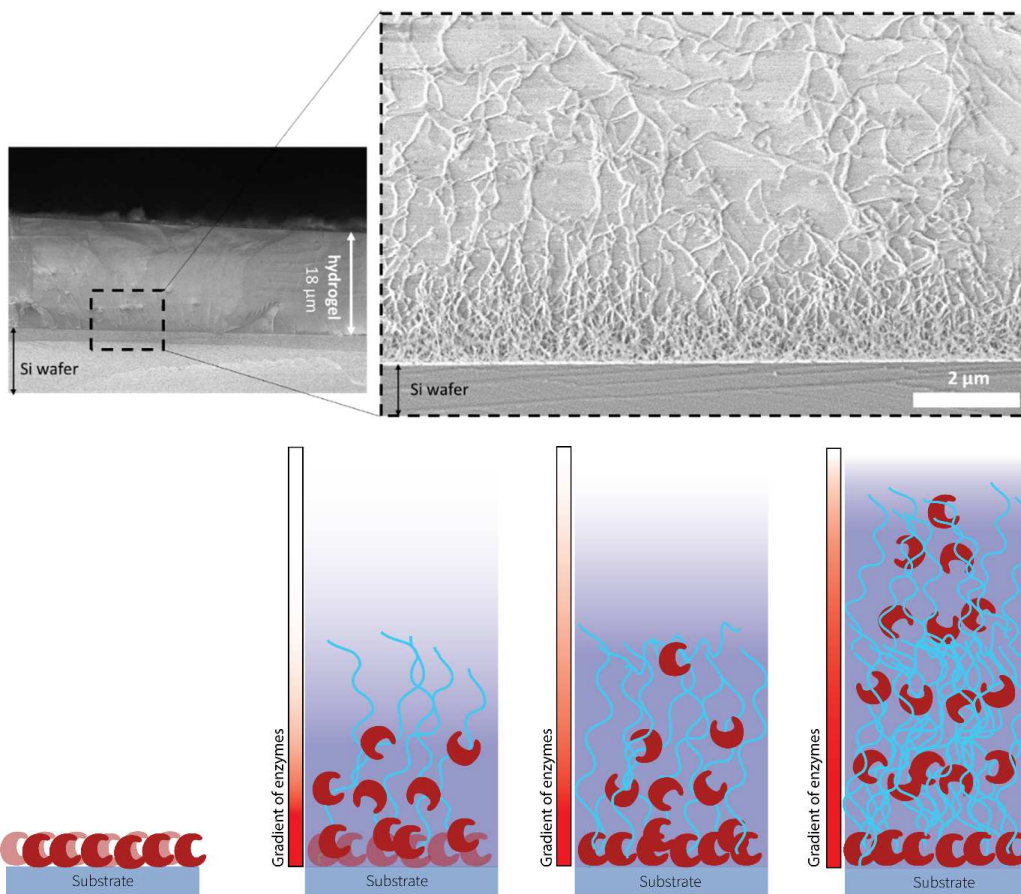


Figure 8. (Top) Typical cryo-SEM image of supramolecular hydrogel grew up from the Fmoc-GFFYGHY self-assembly. This hydrogelator is produced in close vicinity of the surface modified with AP, brought in contact with the dephosphorylated peptide Fmoc-GFFYpGHYp. Reproduced from reference [29] with permission from Wiley-VCH. (Bottom) Schematic of the successive steps going from the enzymes (red croissant) adsorption to the localized self-assembly of LMWH enzymatically produced. The self-assembled fibers are perpendicularly oriented to the surface and the enzymes are distributed in a gradient manner from the bottom to the top of the gel.

2-4 LEASA processes on nanoparticles

When using AP-decorated silica nanoparticles (NPs@AP) and the precursor tripeptide Fmoc-FFpY a homogeneous hydrogel is obtained where self-assembled peptide fibers allow the bridging of nanoparticles, as observed by *cryo*-SEM [51]. Surprisingly, changes in the gel morphology could be observed macroscopically after the sample was rested for a few weeks, leading to phase separation between an opaque gel (phase A, Figure 9) and a translucent gel (phase B, Figure 9). Composition study of these gels showed the presence of nanoparticles and peptides nanofibers in both phases, but *Cryo*-SEM imaging revealed important morphological changes between the two-phase structures, with one displaying a high density in fibrous network while the other showed much smaller density. Such an evolution over time is believed to arise both from the attraction between the nanoparticles and from the affinity of the nanofibers for the enzymes present at the surface of the particles.

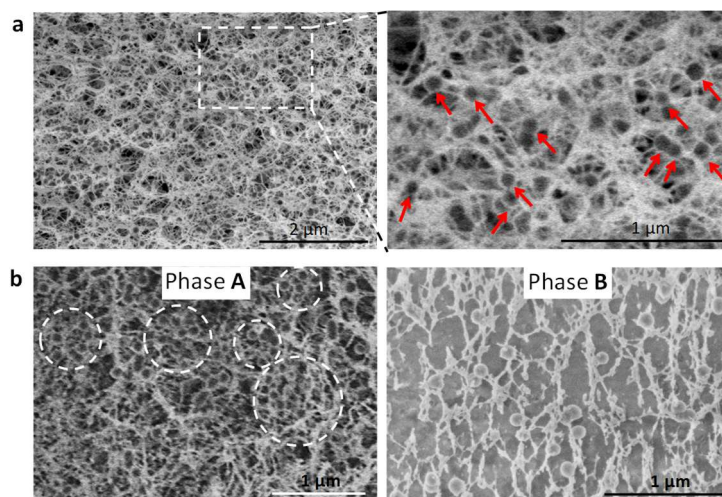
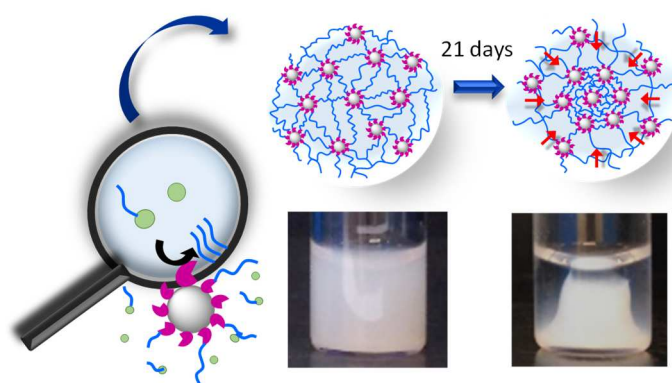


Figure 9. (Top) Fmoc-FFY nanofibers (in blue) self-assembled from AP-modified silica nanoparticles (NPs@AP) by dephosphorylation of Fmoc-FFpY precursor leading to a hybrid supramolecular hydrogel (left picture) undergoing a phase separation over time (right picture). The red arrows show the contraction direction of the gel. (Bottom) Cryo-SEM images of the Fmoc-FFY hydrogel, obtained from a mixture of 1.25% w/v NPs@AP and $1 \text{ mg}\cdot\text{mL}^{-1}$ Fmoc-FFpY, observed after (a) 24 h (left) and zoom-in highlighting single NPs with red arrows (right) and (b) 2 days with the phase A (left) and phase B (right) of the transparent gel phase over time. Reproduced from reference [51] with permission from the American Chemical Society.

Similarly, to the previous example, enzymes were also grafted onto magnetic nanoparticles [47]. Two such systems were elaborated, the first one using thermolysin (system 1) which yielded stable hydrogels and the second one based on chymotrypsin (system 2), similar to the one described earlier (Figure 10). Upon self-assembly, a hub-and-spoke morphology was observed, with nanofibers connecting the nanoparticles together, in both cases. In the first system, only 6% of the initial precursor was converted, which is way less than in examples using thermolysin in solution (ca 70%) but was surprisingly still enough to yield a hydrogel of increased strength. This result is likely to emerge from the high number of enzymes potentially immobilized on each nanoparticle. On the other hand, the second system also displayed an increase in the strength of the hydrogel, but most importantly, a 30-fold increase in the lifetime of the resulting hydrogel. It is proposed that the hub-and-spoke morphology renders peptides less accessible for subsequent hydrolysis, resulting in a higher lifetime. These results show the high importance of the microscopic arrangement for the macroscopic properties of the hydrogels. Moreover, they underline the important versatility of LEASA due to the variety of enzymes that can be used.

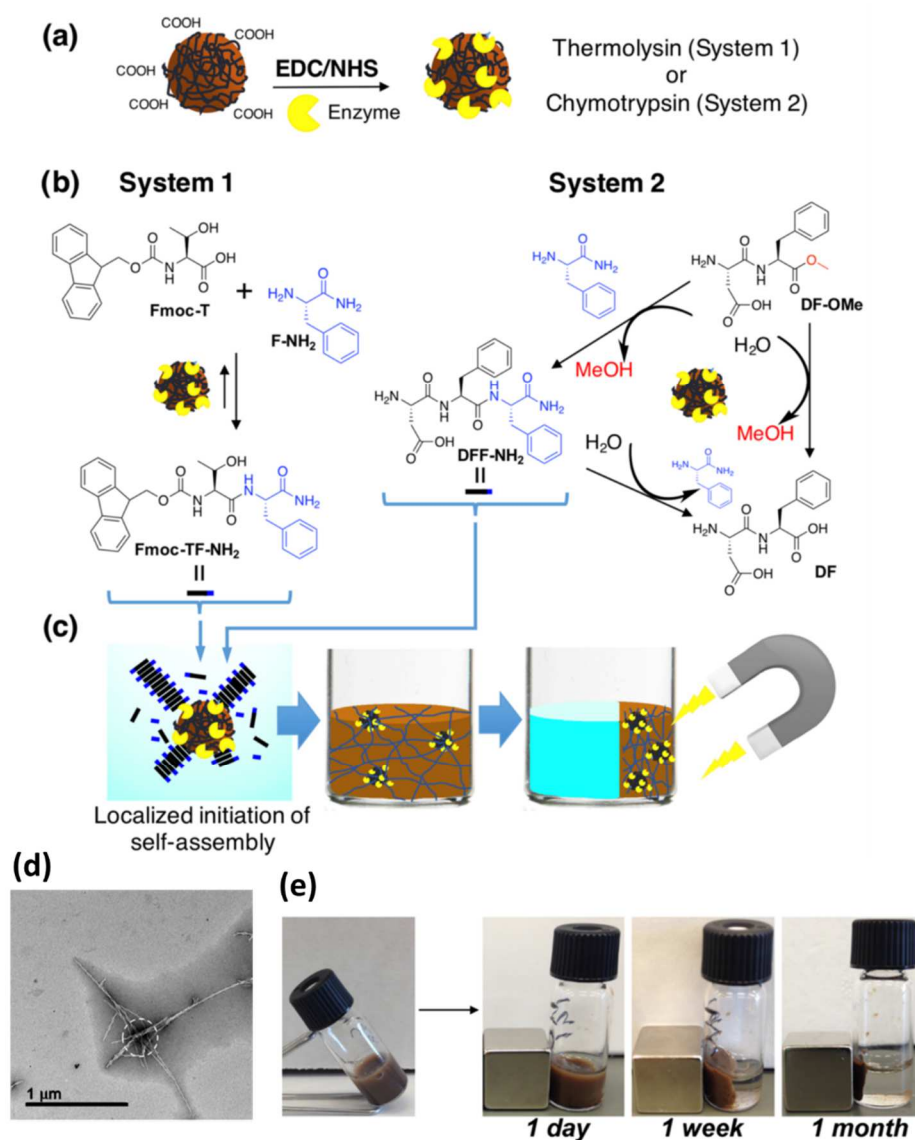


Figure 10. (a) Grafting of enzymes on magnetic nanoparticles using carbodiimide chemistry. (b) Systems 1 and 2 involving thermolysin and chymotrypsin respectively providing the hydrogelator peptide. (c) Schematic of the LEASA process occurring from the magnetic nanoparticles, creating so a peptide self-assembled nanoarchitecture underpinning a supramolecular hydrogel. (d) Hub-and-spoke morphology of nanoparticles decorated by peptide nanofibers around. (e) Picture of the resulting magnetic supramolecular hydrogel and the magnetic field effect overtime. Reproduced from reference [47] with permission from the American Chemical Society.

2-5 LEASA processes in host gels

Hydrogels are soft materials and their manipulation (and thus application) can often be tedious. Consequently, the possibility to embed self-assembled LMWH within a pre-existing, more robust, host materials using LEASA was investigated. In two studies in 2019 [52] and 2020 [53], the formation of an interpenetrated network upon diffusion of adequate peptides into a host hydrogel containing an enzyme was observed. In both reported works, AP was used as the enzyme and Fmoc-FFpY as precursor peptide. Such embedment leads to changes in the hydrogel chemical composition, morphology and in some cases mechanical properties. In the former study, diffusion of a low peptide Fmoc-FFpY concentration solution led to storage moduli lower than the host hydrogel alone. In contrast, higher concentrations of peptides led to an increase of the storage modulus. Similar results could therefore be expected

for the latter contribution based on another hydrogel. However, no significant change in mechanical properties was shown in that case. This is the indication that the possibility to tune the mechanical properties rises from the nature of the host hydrogel. However, importantly, the newly generated peptide hydrogel gave rise to cell-adhesion properties at the surface of the hydrogel, thereby proving that embedment of a secondary network into a host hydrogel using LEASA is an insightful and promising approach towards the tuning of the hydrogel properties. A similar approach was also reported by Mezzenga and coll. in 2019, in which benzaldehyde lyase was used to catalyze the transformation of benzaldehyde into (*R*)-benzoin inside lipidic cubic mesophases (LCMs) [54]. As expected from previous observations, the resulting (*R*)-benzoin underwent self-assembly to form a secondary network inside the primary network. Interestingly, circular dichroism assays revealed significant chiral amplification at high enough concentrations inside of the LCMs as compared to a similar system in solution. Subsequent crystallization was also observed inside the LCMs by polarized optical microscopy (POM). This implies that the self-assembly is merely a kinetically trapped system, slowly evolving towards crystals, which are known to be the most stable state thermodynamically. These results constitute the proof that confined environments can lead to assemblies of higher organization, and consequently that LEASA is a promising strategy for the design of functional systems.

3. Applications of LEASA

3.1. Design of smart materials

Ulijn *et al.* designed a magneto-responsive material using LEASA with enzymes immobilized on the surface of magnetic nanoparticles [47]. After the formation of a self-assembled peptide network between the iron oxide nanoparticles, they investigated the possibility to manipulate the hydrogel by applying an external magnetic field (Figure 10). Remarkably, a resulting contraction of more than 6-fold was observed in the hydrogel volume. Such a contraction resulted in sol-phase exclusion (syneresis). Finally, the magnetic field allowed to “switch off” hydrogel formation when applied in the earliest stage of the LEASA process. Such a macroscopic change in hydrogel structure is reminiscent of the results presented earlier using silica nanoparticles [51]. In that case however, the evolution of the system is time-related, which is of high interest for the emergence of transient and so-called “living” materials. Combining the abilities to tune the mechanical properties of supramolecular hydrogel using LEASA, gives rise to emergent properties (cell adhesion, crystallization...) and controlling the behavior of the material with stimuli or the evolution over time is the key to the design of applicable smart materials. Being involved in all parts of the process, LEASA is therefore a very promising strategy for that purpose.

3.2. LEASA for the design of catalytic systems

3.2.a. LEASA allows the design of supported-hydrogels in flow reactors

Depending on the peptide sequence of the hydrogelator and its resulting self-assembly, it may give rise to enzyme-like supramolecular hydrogels. Thus, catalytically-active supramolecular hydrogels (CASH) displaying catalytic activity have been investigated and

reported [55-59]. However, these CASH have several disadvantages. Namely, they are often single use, the extraction of the product can be tedious and they often display mechanical strengths too weak for their use in a chemical reactor. In 2019, the possibility to use LEASA on the walls of a porous substrate to grow a CASH that would circumvent these issues was investigated [45]. In this case, the hydrogel was built inside of a cell containing an enzyme-coated polymer foam. Remarkably, the resulting hydrogel displayed esterase-like activity towards a range of different non-activated esters, resulting in very high yields in just a few minutes by simple diffusion of the ester solution through the cell. Moreover, enantioselectivity was also shown using this supported-CASH, thus resulting in an enantiopure product from a racemic mixture as observed through chiral HPLC analysis. Finally, the CASH was connected to a flow reactor (Figure 11) and could be reused and stored for several months without any loss in efficiency. This example is the proof that using LEASA, typical problems encountered in the use of CASH can be avoided. Indeed, the presented CASH displayed increased robustness, which allowed its introduction in a chain-reactor allowing for multiple use. Furthermore, this CASH showed high reliability, being stable over months. All together, these properties show the remarkable applicability of LEASA for the bottom-up design of chain-reactors. It must be noted that, because LEASA leads to enzymes strongly immobilized in the resulting hydrogel, supported-CASH exploiting their inherent enzymatic activity in continuous flow applications has never been reported. Very recently, it has been shown that peptide hydrogels enhance the lifetime of oxidases allowing a recyclability of this enzymatically-active materials [60]. Moreover, multiple catalysis including both the enzymatic and catalytic activity rising from the self-assembled network would be interesting as well.

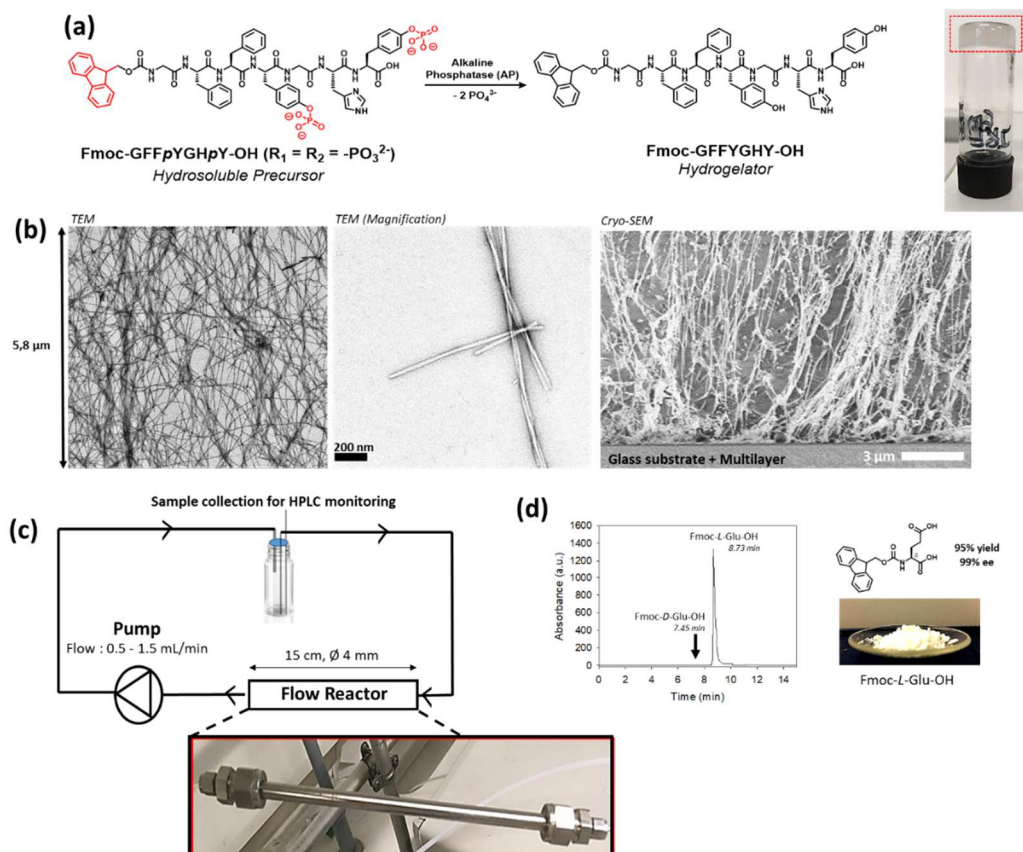


Figure 11. (a) Precursor peptide transformed by AP in hydrogelator. (right) Picture of the corresponding hydrogel. (b) Electronic microscopy images: (left and center) TEM image of the peptide self-assembled nanofibers, (right) z-section cryo-SEM image of a hydrogel grew from a glass substrate initially modified with

AP using a multilayer film. (c) Schematic of the flow reaction containing a CASH-supported polymer foam within a metallic tube (picture). (d) Kinetic resolution of the racemic substrate Fmoc-Glu-OtBu resulting in 95% yield ($\approx 100\text{mg}$) of Fmoc-L-Glu 99% of enantiomeric excess (ee). Reproduced from reference [45] with permission from the Wiley-VCH.

3.2.b. Design of localized supramolecular autocatalytic systems

We have seen that LEASA processes are initiated by enzymes present on a surface. We have also seen that one can design peptide self-assemblies with catalytic properties. These two approaches have been combined to design localized self-assemblies that grow in an autonomous way. [29] Based on two precursors Fmoc-GFFY p GHY p (precursor phosphorylated HP²) and diester homologue having the same peptide sequence but with ester groups instead of the phosphorylated ones (precursor esterified) HE², the system was able to undergo hydrogelation of Fmoc-GFFYGHY (H) in the presence of only attomolar quantities of AP. Dephosphorylation of HP² into H by AP gave rise directly to H self-assembly that displayed esterase properties and was thus, in turn, able to catalyze the transformation of HE² into H, thereby generating an autocatalytic ability. By immobilizing AP onto substrates, subsequent hydrogelation was observed at LMWH concentrations ten times lower than the critical gelation concentration (CGC) as a result of the out-of-equilibrium localized accumulation of LMWH. Examples of such autocatalytic supramolecular systems being scarce, these results are of high importance for the design of new life-like materials.

3.3. Biomedical developments

In vitro design using LEASA for *in vivo* injection and biomedical applications was investigated. First, in 2011 by Williams *et al.* in a study already mentioned previously where the self-assembly was initiated by the presence of laminin [49]. The hydrogel obtained could be microinjected locally into a dystrophic zebrafish model organism in order to deliver the guest protein in laminin-deficient parts of the extra cellular matrix. Importantly, the biomaterial remained stable and confined in space over several days. In this case, the importance of LEASA is that the injected hydrogel is enzyme-free, as the enzymes remained attached to the glass surface upon aspiration of the hydrogel with the syringe, thus avoiding orthogonal processes.

One of the current axes of research for cancer therapy is the use of reactive oxygen species (ROS), bioinspired by neutrophils. ROS, in particular singlet oxygen, have high reactivity and therefore display cytotoxicity. With that strategy in mind, Wu *et al.* developed in 2019 a hybrid self-assembled nanogel mimicking neutrophil lysosomes [61]. To build such a nanogel, AP-coated iron oxide nanoparticles were put in contact with N-Fmoc-protected Tyr-phosphate, *i.e.* Fmoc- p Y. Similarly, to earlier examples, subsequent self-assembly was obtained around the nanoparticles. To catalyze the formation of singlet oxygen, the nanogel was loaded with superoxide dismutase (SOD) and chloroperoxidase (CPO) enzymes which are well known to result in cascade reaction from superoxide radicals -present in tumor cells- to hypochlorous acid and most importantly, singlet oxygen. As a result of injection of this nanogel into animals, remarkable cytotoxicity was observed for cancer cells, whereas healthy cells mostly remained unaffected.

The presence of hyaluronic acid (HA) during the self-assembly process of peptides impacts strongly the mechanical properties of the resulting hydrogel.[62] This was explained by the interaction of HA with the self-assembled Fmoc-FFY nanofibers resulting in micrometer-scale helical fibrils [63]. Localizing AP on glass substrate in presence of Fmoc-FFpY, a several micrometer thick hydrogels were formed for 2D cell culture. It was shown that the presence of HA in the supramolecular material enhances the cell adhesion and cell spreading. When AP is localized on stellate mesoporous silica nanoparticles, a supramolecular hydrogel layer based on Fmoc FFY was generated all around. This soft coating allows the loading of an anticancer agent that can be released through a thermal control.[64]

LEASA systems applied *in vivo* for biomedical applications have been reported previously [65,66]. Taking advantage of the natural expression of an enzyme in a biological environment, this insightful approach allows for promising properties regarding extracellular matrix treatment and cancer therapy. Already being the topic of an existing review by Bing Xu and collaborators [67], it will not further be described here. However, the examples described earlier in this review are the proof that LEASA can serve as an effective approach for the *in vitro* build-up of biomedical solutions and as an alternative to the use of biologically expressed enzymes. We have no doubt that, considering LEASA's versatility, many more insightful treatments are yet to be developed and result in significant progress in various fields of medicine.

4. Perspectives for LEASA

The rate of scientific publications on the study or application of supramolecular hydrogels has increased considerably over the last ten years. Because of the inherent properties of the hydrogels formed, *i.e.* highly hydrated, very soft and generally self-healing, a significant part of these scientific contributions concerns the field of life sciences and biomedicine.[61-67] Among the different stimuli to trigger the LMWH self-assembly processes leading to hydrogel formation, the use of enzymes lies on a special place for two reasons: (i) the biocatalytic action takes place very rapidly at room temperature and (ii) the localization of the enzyme allows controlling where the self-assembled nanofibrous network will form and grow. The application of the LEASA concept thus leads to the formation of a micrometric thick hydrogel coating. In addition, by controlling the enzyme surface density or by using localized seeding nucleation sites of self-assembly, it is also possible to control when the hydrogel will form and its growth rate over time. Finally, the morphology of the resulting nanostructures and their density can also be modulated, changing so the mechanical properties of the materials.

Despite many investigations, several fundamental questions concerning the formation and properties of these supramolecular hydrogels remain unaddressed (Scheme 3): this is the case about the localization of enzymes within these materials and their robust anchoring. Since they induce the assembly of LMWH, they seem to remain within the material formed. Are these enzymes really part of the self-assembled nanostructures, as expected? If so, why has their presence never been demonstrated on these self-assemblies? On the other hand, it has been shown that the nature of the enzyme itself influences the morphology (fiber, ribbon, helix, etc.) of the self-assembled edifice: what are the interactions between the enzymes and the hydrogenators? How does the precursor compound play a role in the initiation of the

assembly process? Are the enzymes able to move in or on the self-assembled architecture? The growth of supramolecular hydrogels from a solid-liquid interface results in the formation of a micrometer-thick film only if the enzymes are adsorbed through weak interactions and not covalently bound to the surface. The internal structure of these gels shows a gradient of nanofibers oriented perpendicularly from the interface to the top of the gel. How can this spatial organization be explained? How are the enzymes distributed in this organization? Even if the answers to these questions do not prevent the use of these localized supramolecular hydrogels in applications, they should nevertheless allow the refinement of their properties.

As mentioned earlier, works on supramolecular hydrogel coatings for applications in the field of controlled release of bioactive compounds, biomaterial design and tissue engineering are already well underway. Undoubtedly, the understanding of the influence of (bio)polymers, proteins, or other compounds (several hydrogenators, growth factors, adhesion ligands) in the formation of the hydrogel will allow to further optimize the performance of these materials, both in their interaction with living organisms and in their chemical and physical stability over long time scales. More recently, it has been shown that these supramolecular hydrogels are particularly suitable for cellular studies in 3D environments [68]. It is likely that the number of investigations in this field will considerably increase in the coming years. Although this aspect is outside the scope of this review, it is worth mentioning here that the localization of self-assembly processes within living systems using endogenous enzymes is a potential therapeutic avenue for the treatment of cancers [11,13], which will certainly see strong development in the future.

The generation of a secondary network of self-assembled LMWHs has recently been illustrated by the diffusion of precursors within host chemical hydrogels encapsulating enzymes [51,52]. The continuation of these reaction-diffusion investigations should lead to the autonomous microstructuration of materials from purely organic compounds and LEASA processes in host-gels constitute one possible way to achieve such microstructuration.

Last but not least, another field of application of these hydrogels that will probably develop considerably concerns catalysis and more generally the development of chemical reactors using catalytically-active supramolecular hydrogel. Indeed, Escuder and van Esch have demonstrated the potential of these hydrogels for efficient and selective chemical transformations [55,56,58]. The ability to support these catalytic hydrogels using LEASA concept highlights that these materials can be used in continuous flow devices.[45] Indeed, the encapsulation of enzymes within supramolecular hydrogels stabilizes these biocatalysts allowing for prolonged use.[60]

Acknowledgements

This work was supported by the Agence Nationale de la Recherche (project “EASA” ANR-18-CE06-0025-03 and project “CASH” ANR-21-CE06-0033), the Fondation pour la Recherche en Chimie through the Labex Chimie des Systèmes Complexes (Project number PSC-016) and the Region Grand-Est (Project MIPPI 4D).

References

- [1] Yang Z, Gu H, Fu D, Gao P, Lam JK, Xu B. *Adv Mater* 2004;16:1440-1444.
- [2] Shy AN, Li J, Shi J, Zhou N, Xu B. *J Drug Target* 2020;760-765.
- [3] Liang C, Yan X, Zhang R, Xu T, Zheng D, Tan Z, Chen Y, Gao Z, Wang L, Li X, Yang Z. *J Control Rel* 2020;337:109-117.

- [4] Liang C, Zheng D, Shi F, Xu T, Yang C, Liu J, Wang L, Yang Z. *Nanoscale* 2017;9:11087-11993.
- [5] Kim BJ, Fang Y, He H, Xu B. *Adv Health Mat* 2021;10:2000416.
- [6] Liu S, Xu B. *ACS Omega* 2020;5:15771-15776.
- [7] Du X, Zhou J, Shi J, Xu B. *Chem Rev* 2015;115:13165-13307.
- [8] Williams RJ, Smith AM, Collins R, Hodson N, Das AK, Ulijn RV. *Nat Nanotechnol* 2009; 4: 19-24.
- [9] Vigier-Carriere C, Wagner D, Chaumont A, Durr B, Lupattelli P, Lambour C, Schmutz M, Hémmérlé J, Senger B, Schaaf P, Boulmedais F, Jierry L. *Langmuir* 2017; 33:8267-8276.
- [10] Yang ZM, Liang G, Ma M, Gao Y, Xu B. *Small* 2007; 3:558-562.
- [11] Wang JY, Li H, Xu B. *RSC Chemical Biology* 2021;2:289-305.
- [12] Kim BJ, Xu B. *Bioconjugate Chemistry* 2020;31:492-500.
- [13] Shi JF, Xu B. *Nano Today* 2015;10:615-630.
- [14] Zhan J, Cai Y, He S, Wang L, Yang Z. *Angew Chem Int Ed* 2018;130:1831-1834.
- [15] Qin X, Xie W, Tian S, Cai J, Yuan H, Yu Z, Butterfoss GL, Khuong AC, Gross RA. *Chem Commun* 2013;49:4839-4841.
- [16] Pappas CG, Shafi R, Sasselli IR, Siccardi H, Wang T, Narang V, Abzalimov R, Wijerathne N, Ulijn R V. *Nat Nanotechnol* 2016;11:960-968.
- [17] Rodon Fores J, Mendez MLM, Mao X, Wagner D, Schmutz M, Rabineau M, Lavallo P., Schaaf P, Boulmedais F, Jierry L. *Angew Chem Int Ed* 2017;56,15984-15988.
- [18] Williams RJ, Gardiner J, Sorensen AB, Marchesan S, Mulder R J, McLean KM, Hartley PG. *Aust J Chem* 2013;66:572-578.
- [19] Yang Z, Xu B. *Chem Commun* 2004;21:2424-2425.
- [20] Thornton K, Abul-Haija YM, Hodson N, Ulijn RV. *Soft Matter* 2013;9:9430-9439.
- [21] Yi M, Guo J, He H, Tan W, Harmon N, Ghebreyessus K, Xu B. *Soft Matter* 2021; 17:8590-8594.
- [22] Rodon Fores J, Criado-Gonzalez M, Schmutz M, Blanck C, Schaaf P, Boulmedais F, Jierry L. *Chem Sci* 2019;10:4761-4766.
- [23] Zhou J, Du X, Li J, Yamagata N, Xu B. *J Am Chem Soc* 2015;137:10040-10043.
- [24] Baillet J, Gaubert A, Verget J., Latxague L, Barthélémy P. *Soft Matter* 2020;16:7648-7651.
- [25] Martin AD, Wojciechowski JP, Robinson AB, Heu C, Garvey CJ, Ratcliffe J, Waddington LJ, Gardiner J, Thordarson P. *Sci Rep* 2017;7:43947.
- [26] Wang Z, Liang C, Shang Y, He S, Wang L, Yang Z. *Chem Commun* 2018; 54:2751-2754.
- [27] Smith AM, Williams RJ, Tang C, Coppo P, Collins RF, Turner ML, Saiani A, Ulijn RV. *Adv Mater* 2008;20:37-41.
- [28] Hughes M, Xu HX, Frederix P, Smith AM, Hunt NT, Tuttle T, Kinloch IA, Ulijn RV. *Soft Matter* 2011;7:10032-10038.
- [29] Rodon Fores J, Criado-Gonzalez M, Chaumont A, Carvalho A, Blanck C, Schmutz M, Boulmedais F, Schaaf P, Jierry L. *Angew Chem Int Ed* 2020;59:14558-14563.
- [30] Deng X, Llamazares AG, Wagstaff JM, Hale VL, Cannone G, McLaughlin SH, Kureisaite-Ciziene D, Löwe. *J Nat Microbiol* 2019;4:2357-2368.
- [31] Hirst AR, Roy S, Arora M, Das AK, Hodson N, Murray P, Marshall S, Javid N, Sefcik J, Boekhoven J, van Esch JH, Santabarbara S, Hunt NT, Ulijn RV. *Nat Chem* 2010;2:1089-1094.
- [32] Vigier-Carriere C, Garnier T, Wagner D, Lavallo P, Rabineau M, Hémmérlé J, Senger B, Schaaf P, Boulmedais F, Jierry L. *Angew Chem Int Ed* 2015;54:10198-10201.
- [33] Li D, Wang H, Kong D, Yang Z. *Nanoscale* 2012;4:3047-3049.

- [34] Jain R, Pal VK, Roy S. *Biomacromolecules* 2020; 21:4180-4193.
- [35] Draper ER, Adams DJ. *Langmuir* 2019;35:6506-6521.
- [36] El Hamoui O, Gaudin K, Battu S, Barthélémy P, Lespes G, Alies B. *Langmuir* 2021;37:297-310.
- [37] Debnath S, Roy S, Abul-Haija YM, Frederix P, Ramalheite SM, Hirst AR, Javid N, Hunt NT, Kelly SM, Angulo J, Khimyak YZ, Ulijn RV. *Chem-Eur J* 2019;25:7881-7887.
- [38] Frederix P, Kania R, Wright JA, Lamprou DA, Ulijn RV, Pickett CJ, Hunt NT. *Dalton Trans* 2012;41:13112-13119.
- [39] Zhan J, Cai Y, Ji S, He S, Cao Y, Ding D, Wang L, Yang Z. *ACS Appl Mater Interfaces* 2017;9:10012-10018.
- [40] Wang Y, Tang L, Yu J. *Colloid Interface Sci* 2008; 319:357-364.
- [41] Li R, Horgan CC, Long B, Rodriguez AL, Mather L, Barrow CJ, Nisbet DR, Williams RJ. *RSC Adv* 2015;5:301-307.
- [42] Wang Q, Yang Z, Gao Y, Ge W, Wang L, Xu B. *Soft Matter* 2008;4:550-553.
- [43] Roy S, Javid N, Frederix P, Lamprou DA, Urquhart AJ, Hunt NT, Halling PJ, Ulijn RV. *Chem-Eur J* 2012;18:11723-11731.
- [44] Haburcak R, Shi JF, Du XW, Yuan D, Xu B. *J Am Chem Soc* 2016;138:15397-15404.
- [45] Rodon Fores J, Criado-Gonzalez M, Chaumont A, Carvalho A, Blanck C, Schmutz M, Serra C A, Boulmedais F, Schaaf P, Jierry L. *Angew Chem Int Ed* 2019;58:18817-18822.
- [46] Vogt C, Ball V, Mutterer J, Schaaf P, Voegel J-C, Senger B, Lavallo P. *J Phys Chem B* 2012;116:5269-5278.
- [47] Conte MP, Sahoo JK, Abul-Haija YM, Lau K HA, Ulijn RV. *ACS Appl Mater Interfaces* 2018;10:3069-3075.
- [48] Johnson EK, Adams DJ, Cameron PJ. *J Am Chem Soc* 2010;132:5130-5136.
- [49] Williams RJ, Hall TE, Glattauer V, White J, Pasic PJ, Sorensen AB, Waddington L, McLean KM, Currie PD, Hartley PG. *Biomaterials* 2011;32:5304-5310.
- [50] Olive AGL, Abdullah NH, Ziemecka I, Mendes E, Eelkema R, van Esch JH. *Angew Chem Int Ed* 2014;53:4132-4136.
- [51] Criado-Gonzalez M, Fores JR, Carvalho A, Blanck C, Schmutz M, Kocgozlu L, Schaaf P, Jierry L, Boulmedais F. *Langmuir* 2019;35:10838-10845.
- [52] Criado-Gonzalez M, Rodon Fores J, Wagner D, Schroeder AP, Carvalho A, Schmutz M, Harth E, Schaaf P, Jierry L, Boulmedais F. *Chem Commun* 2019;55:1156-1159.
- [53] Criado-Gonzalez M, Loftin B, Fores JR, Vautier D, Kocgozlu L, Jierry L, Schaaf P, Boulmedais F, Harth E. *J Mat Chem B* 2020;8:4419-4427.
- [54] Zhou T, Vallooran JJ, Mezzenga R. *Nanoscale* 2019;11:5891-5895.
- [55] Rodriguez-Llansola F, Escuder B, Miravet JF. *J Am Chem Soc* 2009;131:11478-11484.
- [56] Rodriguez-Llansola F, Miravet JF, Escuder B. *Chem Commun* 2009;47:7303-7305.
- [57] Gao Y, Zhao F, Wang QG, Zhang Y, Xu B. *Chem Soc Rev* 2010;39:3425-3433.
- [58] Singh N, Zhang K, Angulo-Pachon CA, Mendes E, van Esch JH, Escuder B. *Chem Sci* 2016;7:5568-5572.
- [59] Zozulia O, Dolan MA, Korendovych IV. *Chem Soc Rev* 2018;47:3621-3639.
- [60] Ben-Zvi O, Grinberg I, Orr AA, Noy D, Tamamis P, Yacoby I, Adler-Abramovich L. *ACS Nano* 2021;15:6530-6539.
- [61] Wu Q, He Z, Wang X, Zhang Q, Wei Q, Ma S, Ma C, Li J, Wang Q. *Nat Commun* 2019; 10:240.

- [62] Aviv M, Halperin-Sternfeld M, Grigoriants I, Buzhansky L, Mironi-Harpaz I, Seliktar D, Einav S, Nevo Z, Adler-Abramovich L. *ACS Appl Mat Interf* 2018;10:41883-41891.
- [63] Rodon Fores J, Bigo--Simon A, Wagner D, Payrastre M, Damestoy C, Blandin L, Boulmedais F, Kelber J, Schmutz M, Rabineau M, Criado-Gonzalez M, Schaaf P, Jierry L. *Polymers* 2021;13:1793.
- [64] Li B, Criado-Gonzalez M, Adam A, Bizeau J, Mélart C, Carvalho A, Bégin S, Bégin D, Jierry L, Mertz D. *ACS Appl Nano Mater* 2022;5:120-125.
- [65] Pires RA, Abul-Haija YM, Costa DS, Novoa-Carballal R, Reis RL, Ulijn RV, Pashkuleva I. *J Am Chem Soc* 2015;137:576-579.
- [66] Zhang J, Gao J, Chen M, Yang Z. *Antioxid Redox Signal* 2014;20:2179-2190.
- [67] Shy AN, Kim BJ, Xu B. *Matter* 2019;1:1127-1147.
- [68] Saydé T, El Hamoui O, Alies B, Gaudin K, Lespes G, Battu S. *Nanomaterials* 2021;11:421.

